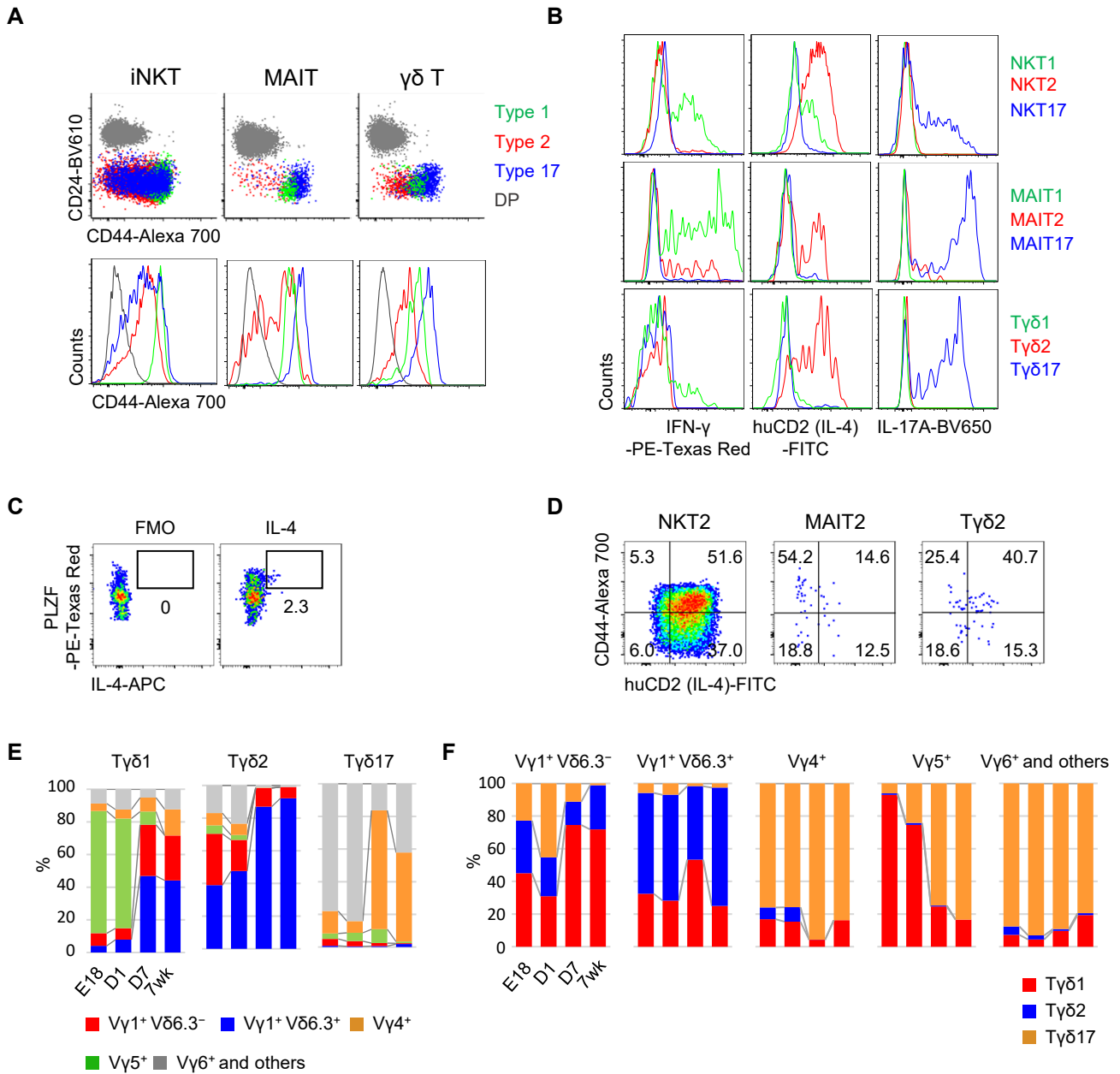


Supplementary information

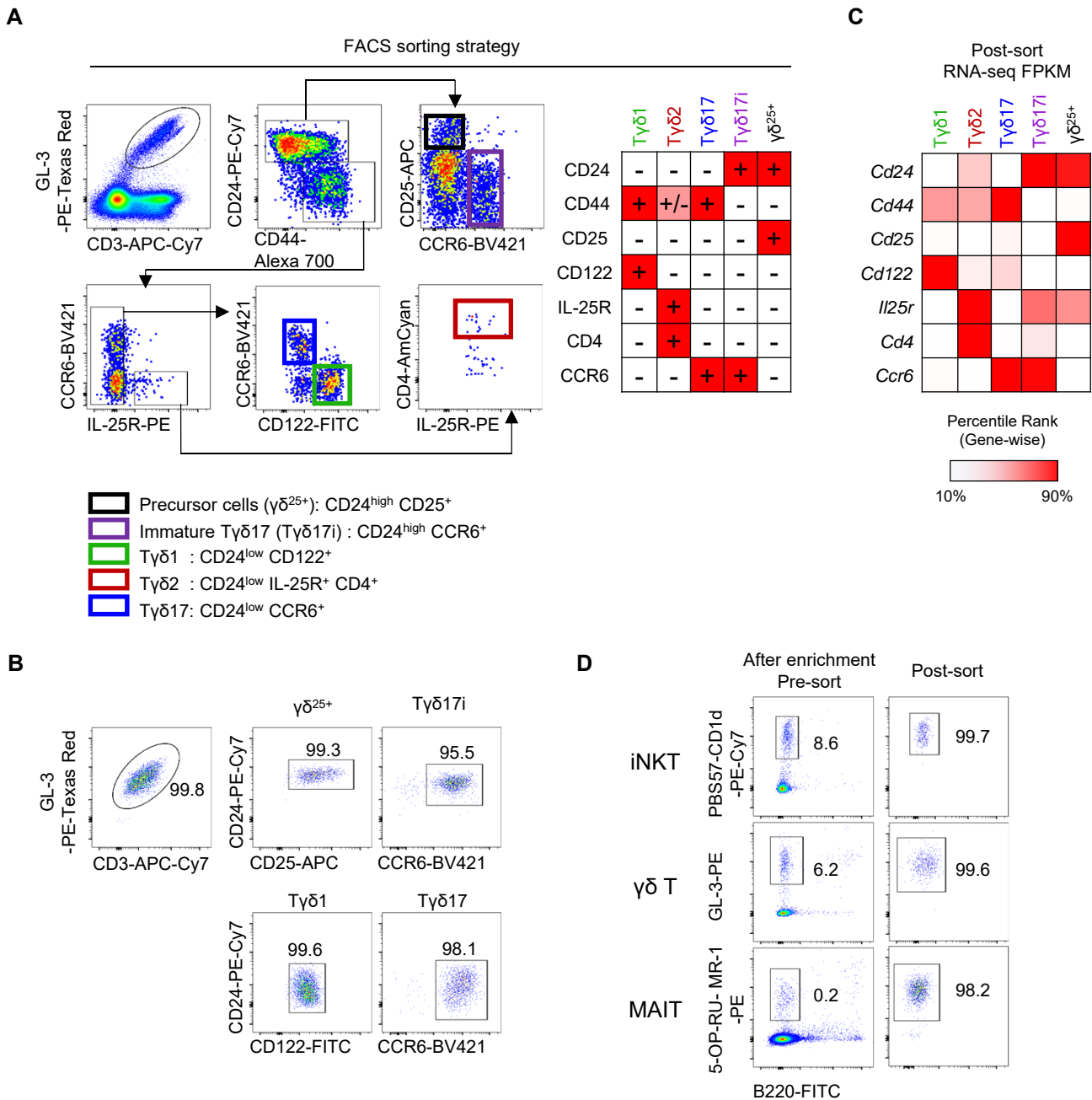
**Single-cell RNA sequencing identifies shared  
differentiation paths of mouse thymic innate T cells**

Lee et al.

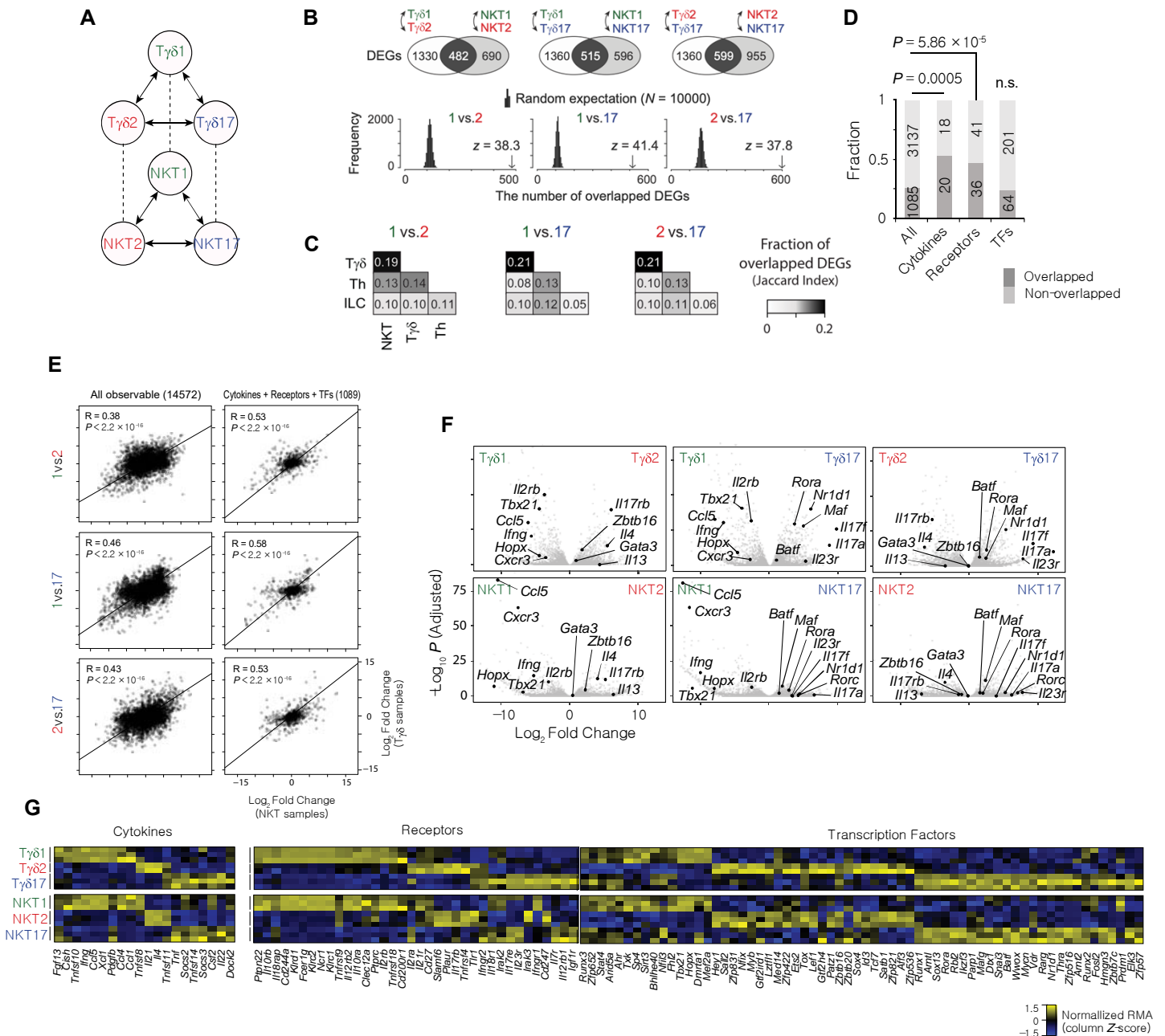
This file contains Supplementary Figures 1-20 and Supplementary Tables 1 and 2.



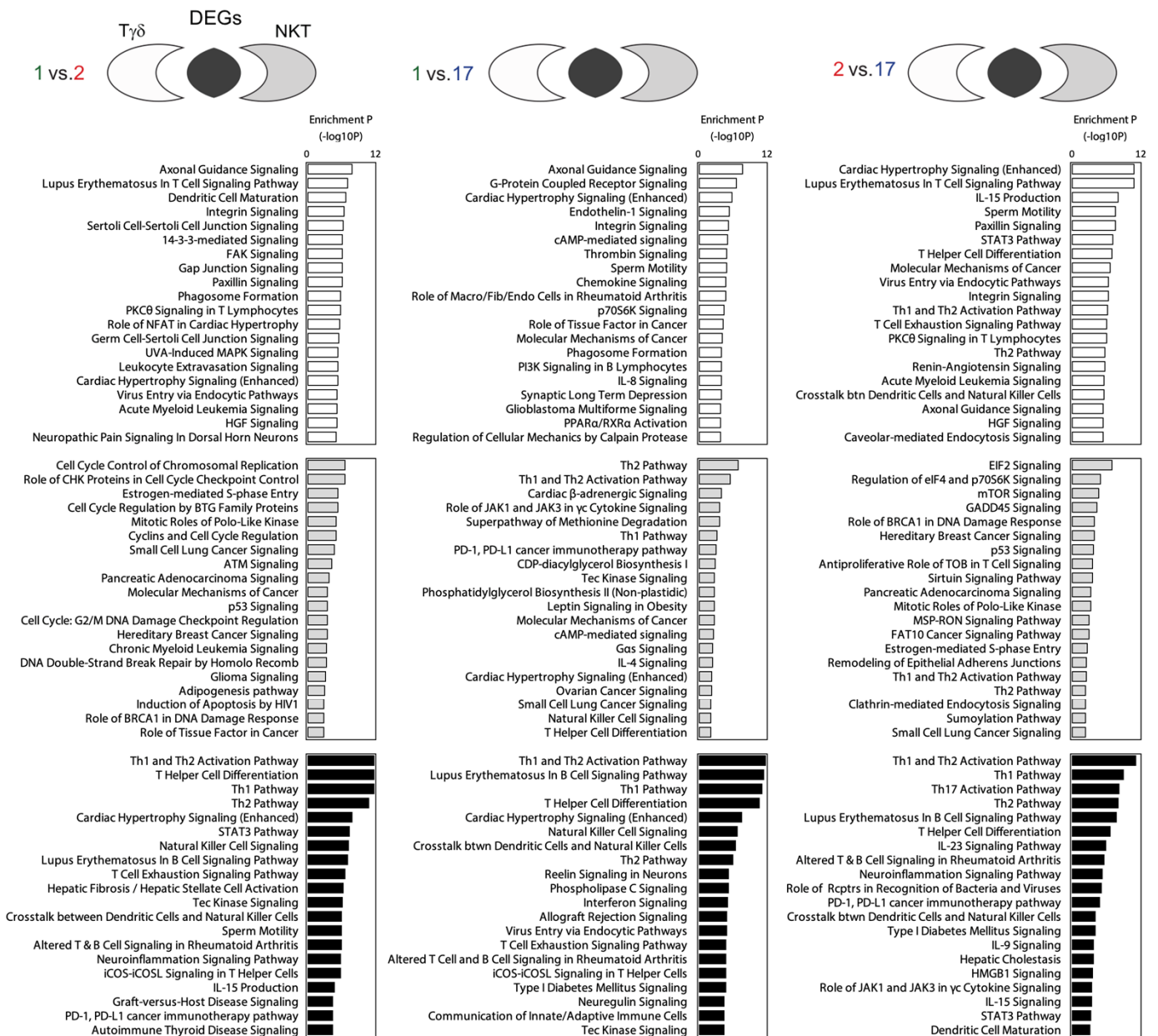
**Supplementary Figure 1. Thymic development of innate T cells.** (A) iNKT, MAIT and  $\gamma\delta$  T subsets gated in Figure 1A were analyzed for their expression of CD24 and CD44. Dot plots and histograms show representative results of at least five different experiments. (B and C) Thymocytes were stimulated with PMA/ ionomycin and indicated subsets gated as in Figure 1A were intracellularly stained with IFN- $\gamma$  and IL-17A or surface stained with human CD2 (huCD2) in KN2 mice (B). CD24<sup>lo</sup> PLZF<sup>+</sup> MAIT cells gated as in Figure 1A were intracellularly stained with IL-4 (C) For MAIT cell cytokine analysis, 6-9 mice were pooled together. Experiments were repeated at least 3 times. (D) Dot plots show correlation between CD44 and huCD2 expressions in indicated cell types of KN2 mice in the thymus. (E and F) T $\gamma\delta$ 1, T $\gamma\delta$ 2 and T $\gamma\delta$ 17 cells defined as shown in Figure 1A were analyzed for their usage of indicated TCR $\gamma\delta$  chains at embryonic day 18 (E18, n=6), postnatal day 1 (D1, n=4), postnatal day 7 (D7, n=4), 7 week-old mice (7wk, n=3). Bar graphs show mean frequencies of indicated subset. Data were pooled from five independent experiments. Source data are provided as a Source Data file.



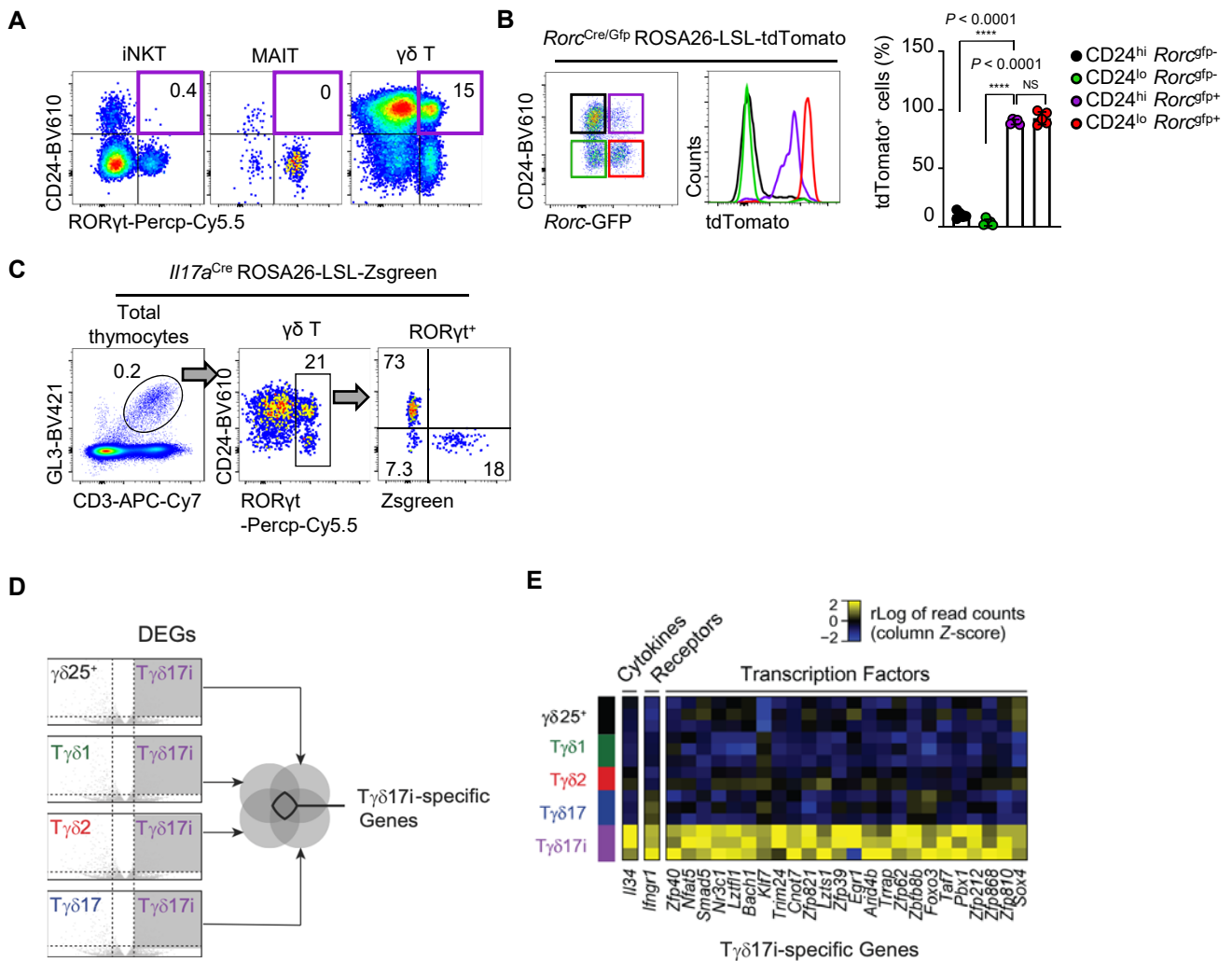
**Supplementary Figure 2. Sorting strategy of  $\gamma\delta$  T cell subsets for bulk and scRNAseq.** (A)  $\gamma\delta$  T cells were enriched from 5 day-old BALB/c thymocytes and stained with indicated markers. Five different subsets were sorted as shown in table and legend. (B) Dot plots show sorting purity of cells used for bulk-RNAseq. (C) Bulk RNA-seq FPKM values of markers used in the cell sorting were analyzed after sorting. (D) Single cell suspensions from thymi of BALB/c mice were enriched with total iNKT,  $\gamma\delta$  T, MAIT cells using MACS (left, pre-sort) and FACS sorted for single cell analysis (right, post-sort). Dot plots show their sorting purities. Numbers indicate frequency of cells in adjacent gates.



**Supplementary Figure 3. iNKT and  $\gamma\delta$  subsets share transcriptional profiles.** (A) Schematic figure depicts comparison strategy of iNKT and  $\gamma\delta$  T transcripts. Solid arrow represents pairwise comparisons of DEGs between subsets and dotted line presents numeric comparison of overlapped DEGs across  $\gamma\delta$  T and iNKT cells. (B) Venn-diagrams present the numeric comparison of overlapped DEGs across iNKT and  $\gamma\delta$  T cells. Bootstrapping analysis with shuffling of DEGs follows to show the statistical significance of the overlap. (C) Fractions of overlapped DEGs, calculated by Jaccard index, were compared among iNKT,  $\gamma\delta$  T, Th, ILC subsets. (D) Fractions of overlapped DEGs were compared among cytokines, receptors, transcription factors (TFs) and other genes.  $P$ -values were calculated with two-sided Fisher-exact test without multiple-test correction. (E) Scatter plots show gene expression ratios ( $\log_2$  of fold-change) between corresponded subsets across iNKT and  $\gamma\delta$  T cells. 'All observable' indicates mouse genes of which expression values are available in all samples. Cytokines + Receptors + TFs are union set of cytokine, receptor and transcription factor genes. (F) Volcano plots were generated after the pairwise comparison of indicated subsets. Genes that are known as DEGs in iNKT subsets were stressed and labeled. (G) Heat maps show expression patterns of cytokines, receptors and TFs mapped to overlapped differentially expressed genes (DEGs) in iNKT and  $\gamma\delta$  T cells.

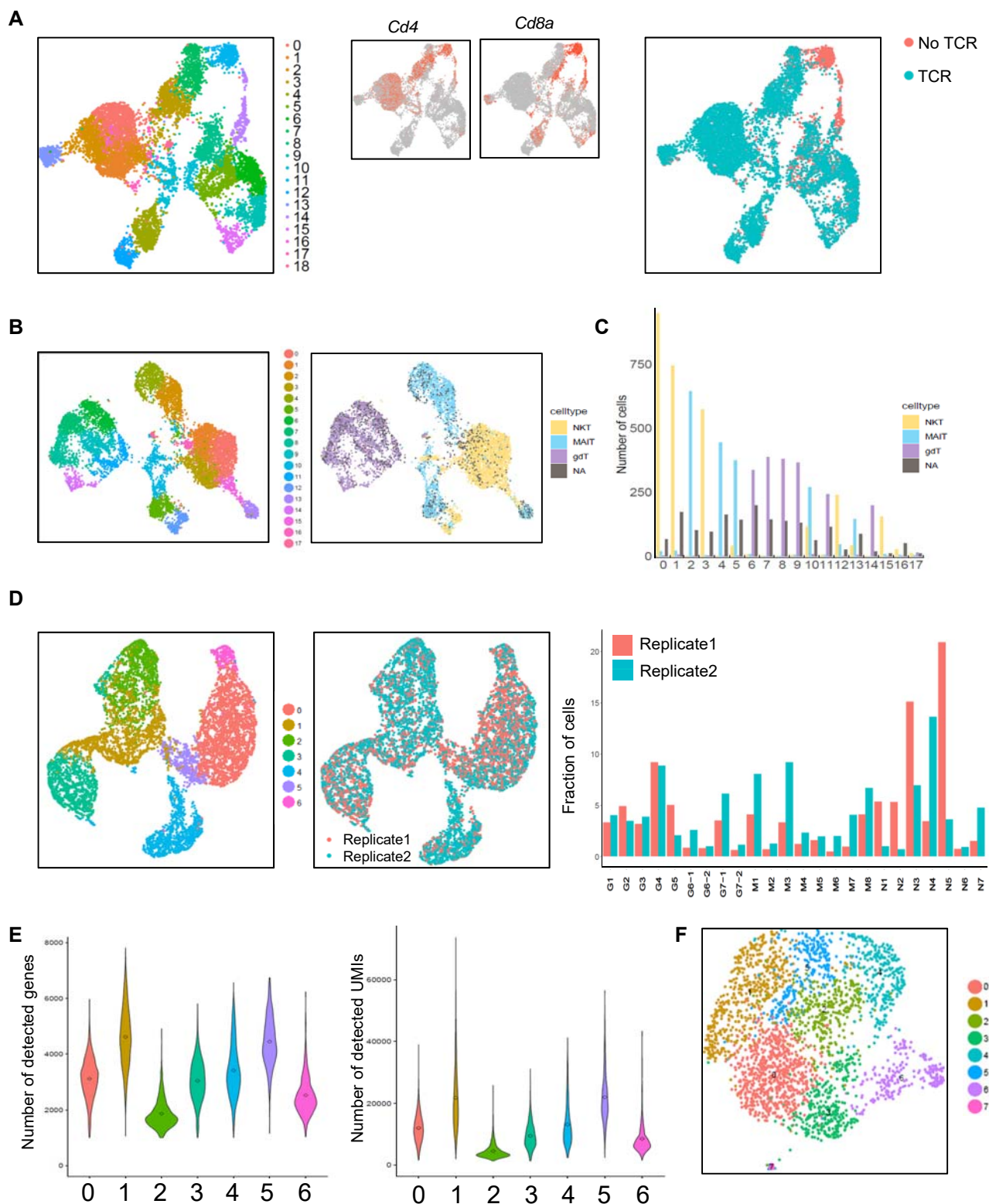


**Supplementary Figure 4. Pathways that are distinct or common between  $\gamma\delta$  T and NKT lineages.** Functional enrichment studies were conducted in common,  $\gamma\delta$ -specific and NKT-specific DEGs between type 1 vs. type 2 (1 vs. 2), type 1 vs. type 17 (1 vs. 17) and type 2 and type 17 (2 vs. 17) subsets. Using IPA analysis, we listed top-20 significantly enriched canonical pathways ( $P < 0.05$ , one-tailed hypergeometric test with multiple-test correction).

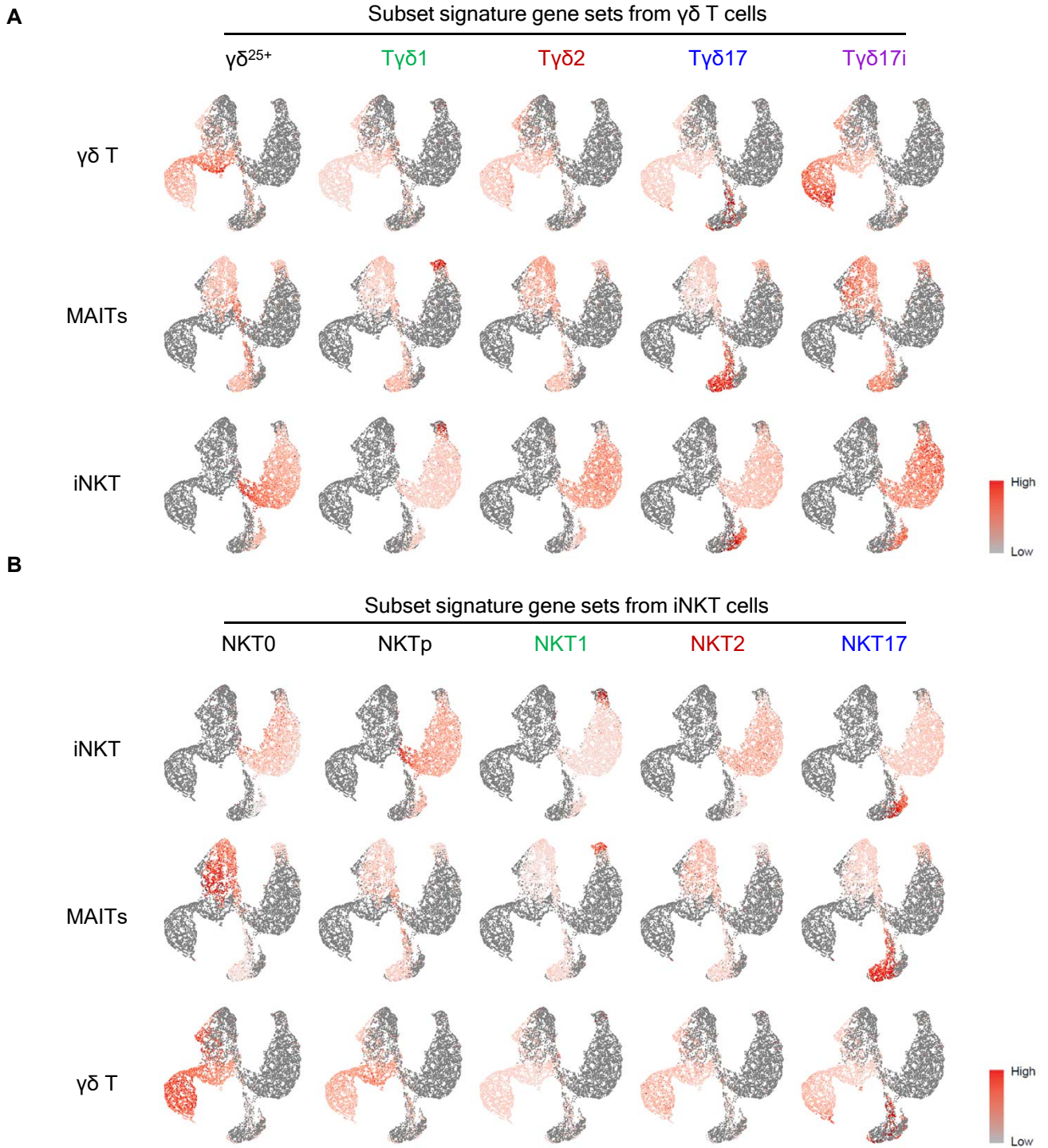


**Supplementary Figure 5. Immature T $\gamma\delta$ 17 cells express ROR $\gamma$ t and have unique transcriptional signature.**

(A) Single cell suspensions of 7 week old BALB/c thymocytes were enriched with iNKT, MAIT and  $\gamma\delta$  T cells using MACS beads. Representative dot plots show CD24 and ROR $\gamma$ t expression patterns of each cell type. Results are from at least five independent experiments. Numbers indicate frequencies of cells in adjacent gates. Data are presented as mean values  $\pm$  SD. Unpaired two-tailed *t*-tests were used for data analysis. \*\*\*\**P*<0.0001. NS, not significant. Source data are provided as a Source Data file. (B) Single cell suspensions of thymocytes from *Rorc*<sup>Cre/Gfp</sup> ROSA26-LSL-tdTomato mice were enriched with  $\gamma\delta$  T cells and analyzed for tdTomato expression in each subset. Representative dot plot and histogram are shown (left) and graph shows statistical analysis of frequencies of tdTomato expressing cells (right, n=5). Results from two independent sets of experiments are shown. (C) Representative dot plots show Zsgreen expression from CD24<sup>+</sup> and CD24<sup>-</sup> ROR $\gamma$ t<sup>+</sup> thymic  $\gamma\delta$  T cells in *I17a*<sup>Cre</sup> ROSA26-LSL-Zsgreen mice. Representative data from three independent experiments are shown. (D and E) T $\gamma\delta$ 17i cells were sorted as showed in supplementary figure 3 and analysed with other  $\gamma\delta$  T subsets. (D) Schematic figure shows how T $\gamma\delta$ 17i-specific genes are generated from volcano plots. T $\gamma\delta$ 17i-specific genes are from the intersection of DEGs overexpressed in T $\gamma\delta$ 17i compared to other  $\gamma\delta$ T subsets. (E) Heat map shows cytokine, receptors and transcription factors in T $\gamma\delta$ 17i-specific genes.

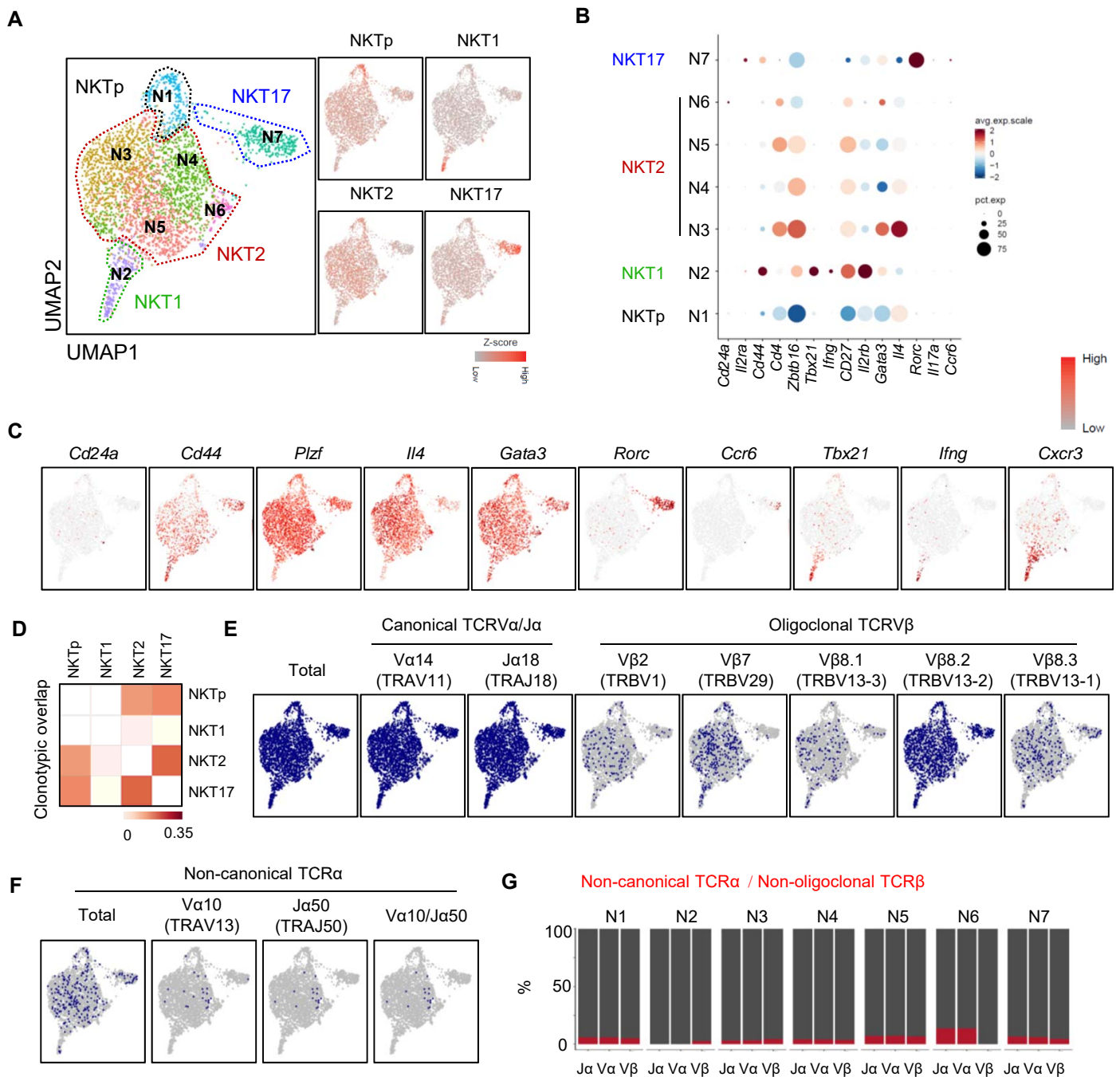


**Supplementary Figure 6. Quality control for scRNA-seq.** (A) UMAP plots show all cells before demultiplexing, which are colored by cell clusters (left), the expression levels of *Cd4* and *Cd8a* (middle) and the presence of detected TCRs (right). (B) UMAP plots of cells after excluding cluster 11 and 14 from (A), colored by reassigned cell clusters (left), demultiplexed cell types (right). (C) Bar plot shows the number of cells assigned to iNKT, MAIT,  $\gamma\delta$  T cells, or unassigned (NA) for each cell cluster. (D) UMAP plots show all assigned cells colored by cell clusters (left), replicates (center). Bar plot shows fractions of cells by replicates for each cell cluster of iNKT, MAIT, and  $\gamma\delta$  T cells (right). (E) Violin plots illustrate the number of detected genes (left) and UMIs (right) per cell for each cell cluster. (F) UMAP plot of  $\gamma\delta$  T cells showing an outlier cluster (cluster 7) which was removed from further analysis.

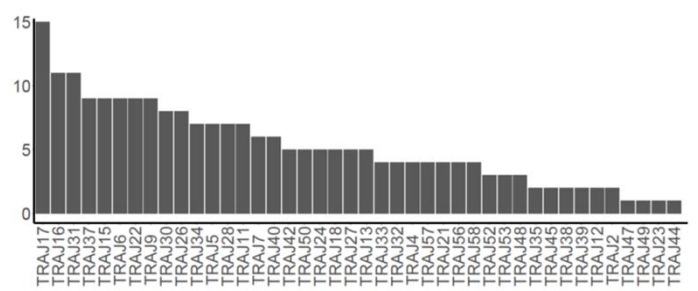
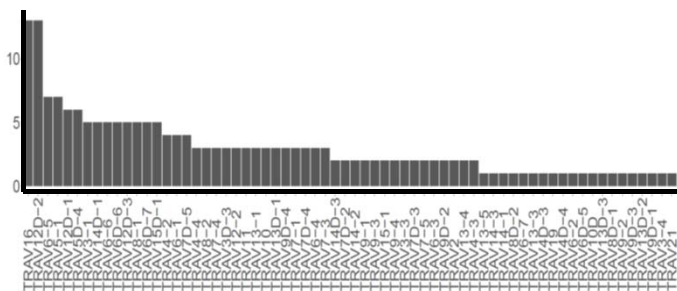
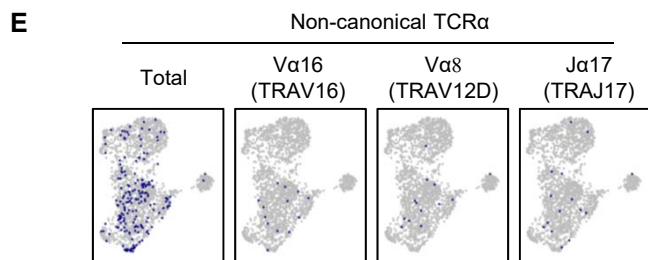
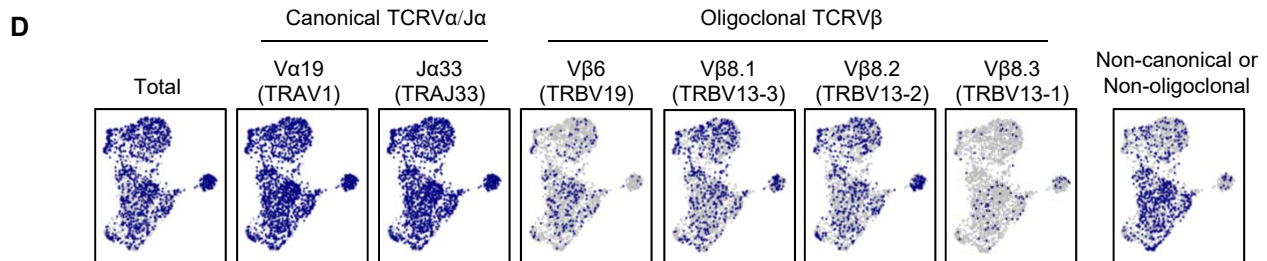
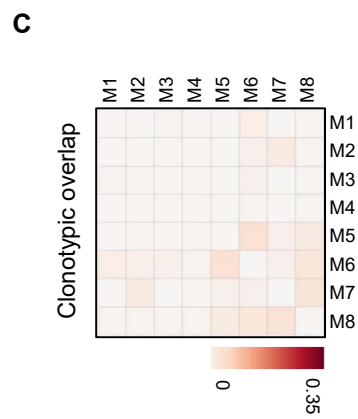
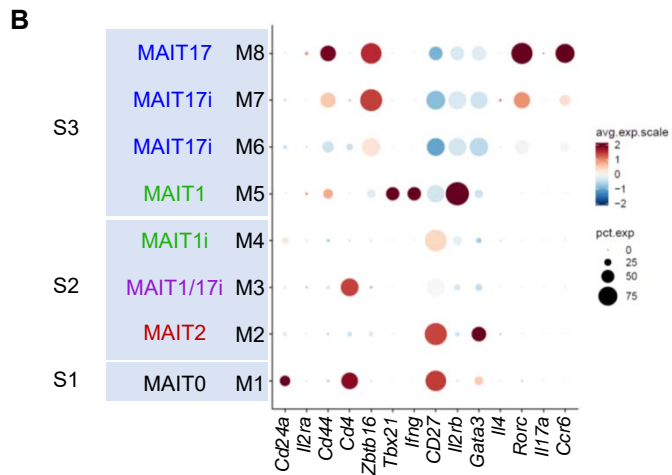
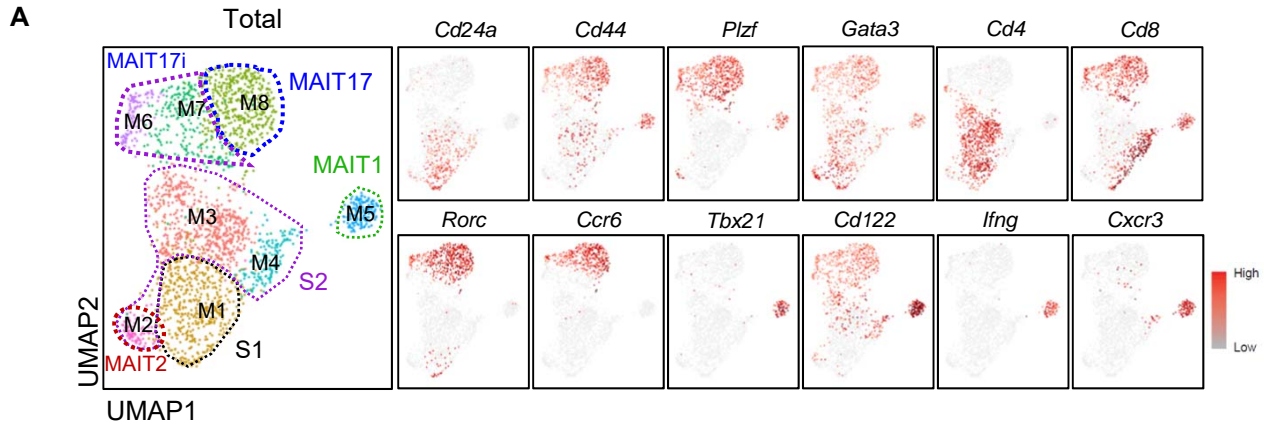


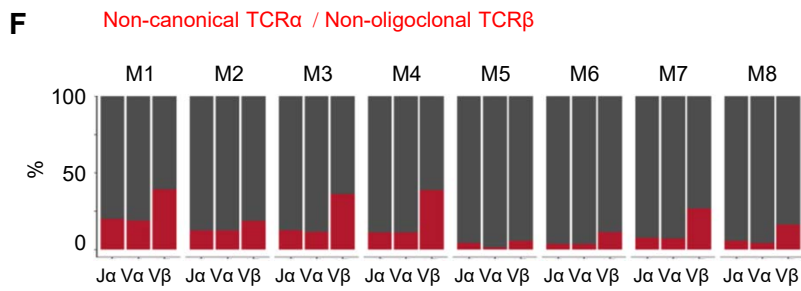
**Supplementary Figure 7. Signature gene expression patterns of innate T cells.** For each type of innate T cells, UMAP plots were colored by the signature scores defined by signature gene sets of functional subsets of  $\gamma\delta$  T cells (A) and iNKT cells (B).



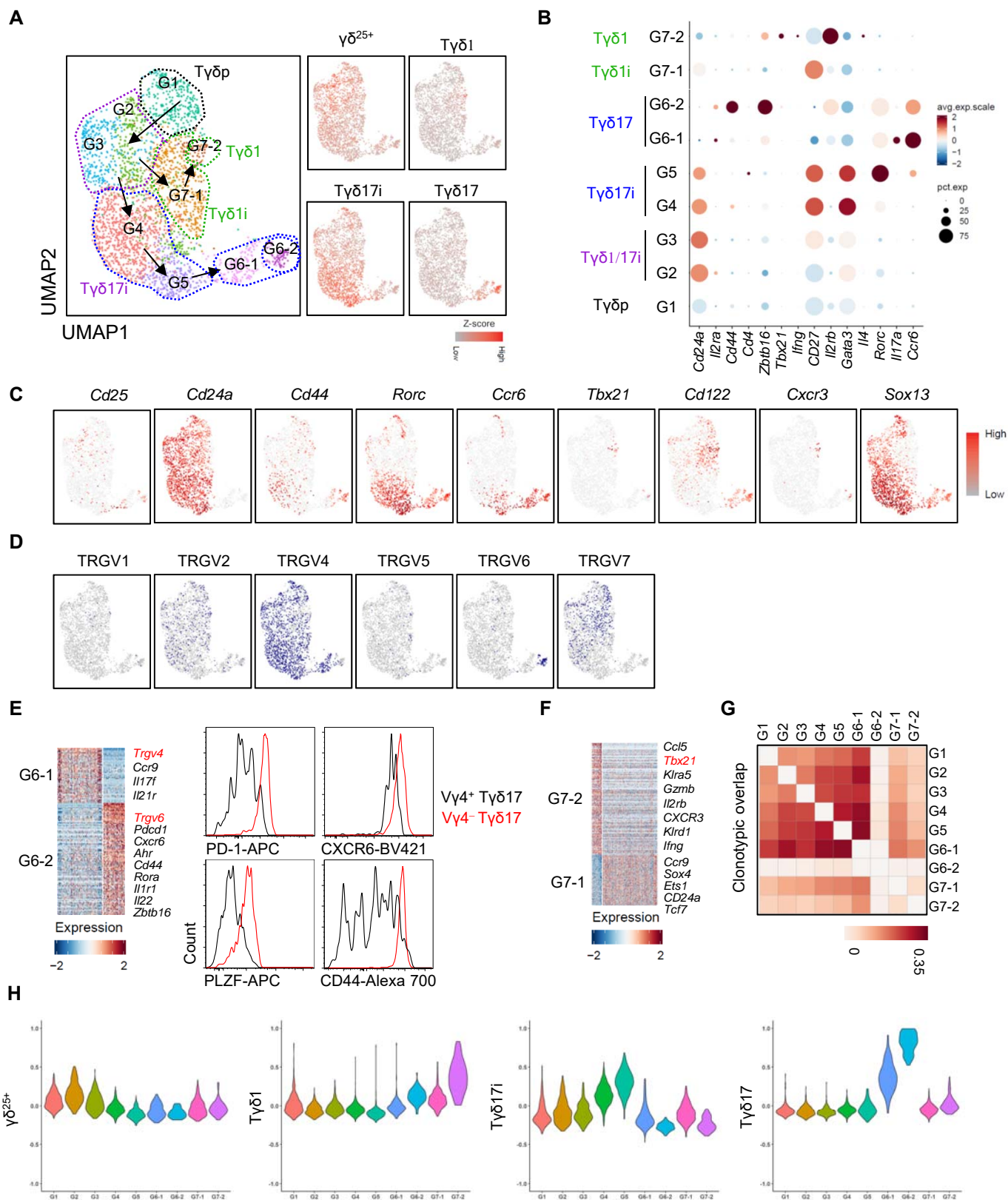


**Supplementary Figure 8. Single cell analysis of iNKT cells.** (A) UMAP plot is color-coded for each cell cluster (left, 1 panel) and signature scores of functional subsets of iNKT cells (right, 4 panels). (B) Dot plot shows the expression levels and frequencies of indicated genes in each cluster. The size and color of the dot represent the percentage of cells expressing the marker gene and the relative expression level (Z-score) within a cell cluster, respectively. (C) UMAP plots are colored by the expression level of indicated genes. (D) Heat map shows geometric mean of total frequencies of clonotypes that overlap between indicated subsets. (E-F) UMAP plots are colored by the presence of indicated TCR genes. (G) Bar graph shows percentage of cells expressing non-canonical TCRV $\alpha$  /J $\alpha$  and non-oligoclonal TCRV $\beta$  chains in each cluster.

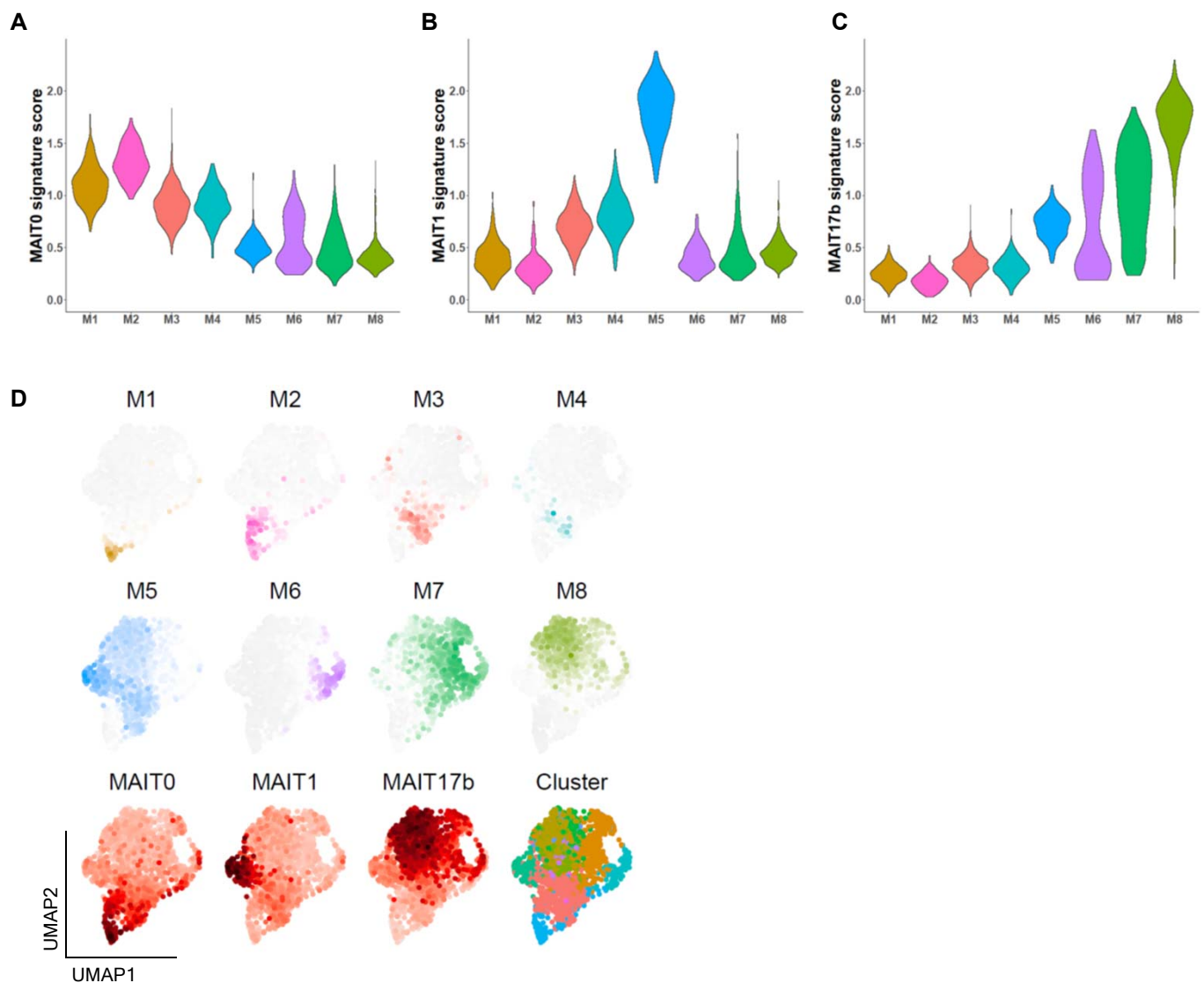




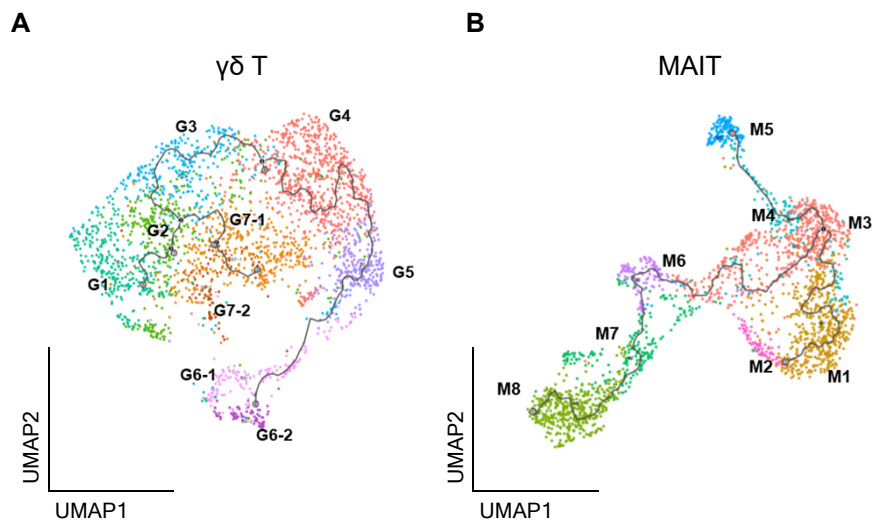
**Supplementary Figure 9. Single cell analysis of MAIT cells.** (A) UMAP plot is color-coded for each cell cluster (left, 1 panel). Expression levels of indicated genes were colored in UMAP (right, 12 panels). (B) Dot plot shows the expression levels and frequencies of indicated genes in each cluster. The size and color of the dot represent the percentage of cells expressing the marker gene and the relative expression level (Z-score) within a cell cluster, respectively. (C) Heat map shows geometric mean of total frequencies of clonotypes that overlap between indicated subsets. (D) UMAP plots are colored by the presence of indicated TCR genes. (E) UMAPs show the presence of indicated TCRs (top) and graphs show the distribution of frequently used non-canonical TCR V $\alpha$  and J $\alpha$  genes (bottom). (F) Bar graph shows percentage of cells expressing non-canonical TCRV $\alpha$  /J $\alpha$  and non-oligoclonal TCR $\beta$  chains in each cluster.



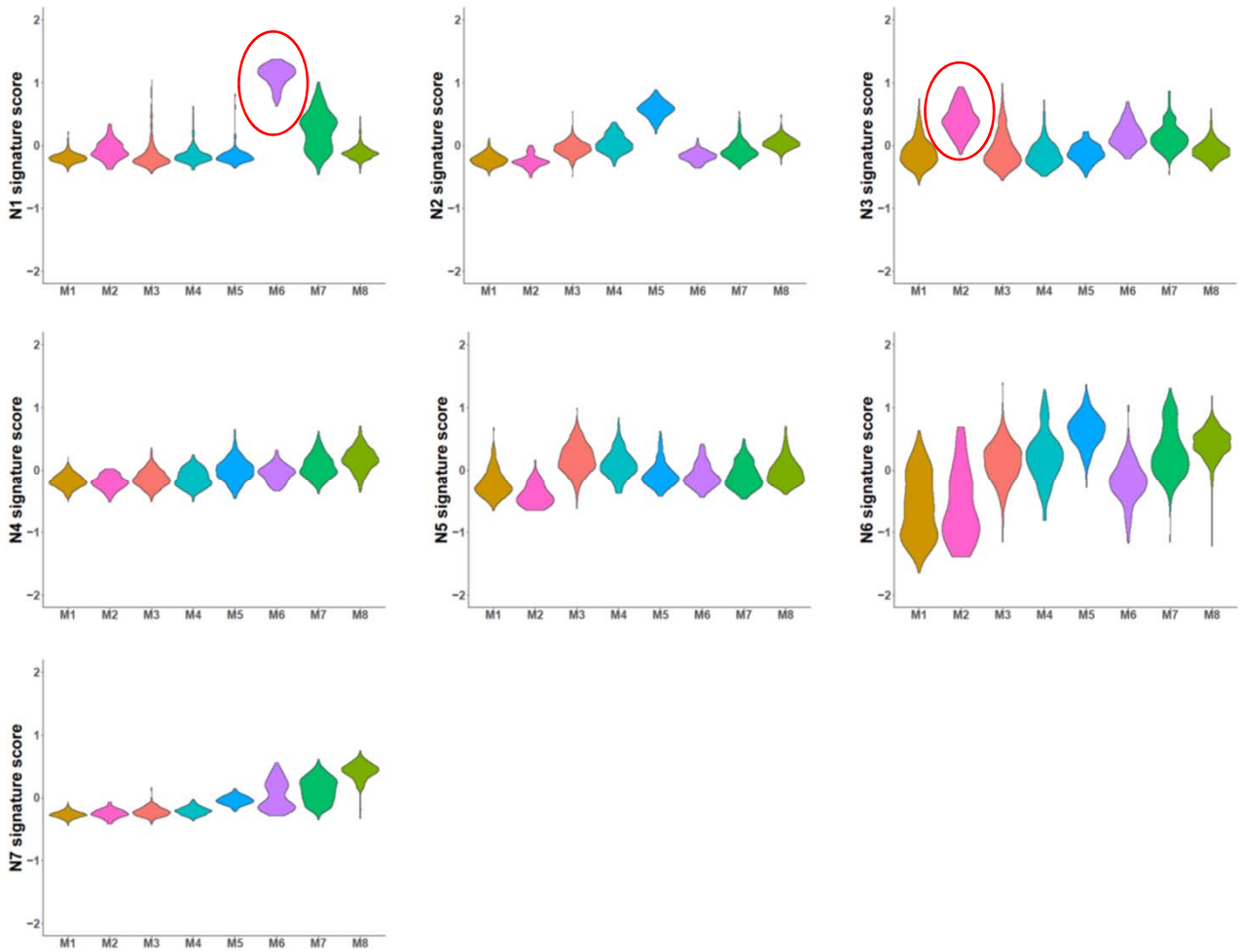
**Supplementary Figure 10. Single cell analysis of  $\gamma\delta$  T cells.** (A) UMAP plot is color-coded for each cell cluster (left, 1 panel) and signature scores of functional subsets of  $\gamma\delta$  T cells (right, 4 panels). (B) Dot plot shows the expression levels and frequencies of indicated genes in each cluster. The size and color of the dot represent the percentage of cells expressing the marker gene and the relative expression level (Z-score) within a cell cluster, respectively. (C) UMAP plots are colored by the expression level of indicated genes. (D) UMAP plots colored by the presence of indicated TRGV genes. (E) Heat map shows the relative expression of differentially expressed genes between G6-1 and G6-2 (left). The histograms show the representative expression profiles of indicated markers on the  $V\gamma 4^+$  or  $V\gamma 4^-$   $T\gamma\delta 17$  cells of BALB/c thymocytes from three independent experiments (right). (F) Heat map shows the relative expression of differentially expressed genes between G7-1 and G7-2. (G) Heat map shows geometric mean of total frequencies of clonotypes that overlap between indicated subsets. (H) Violin plots showing  $\gamma\delta^{25+}$ ,  $T\gamma\delta 1$ ,  $T\gamma\delta 17i$  and  $T\gamma\delta 17$  signature scores for each cell cluster of  $\gamma\delta$  T cells.



**Supplementary Figure 11. Sex difference of MAITs.** (A-C) Violin plots showing MAIT0 (A), MAIT1 (B), and MAIT17b (C) signature scores defined by Legoux et al. (Ref #13) for each cell cluster of MAITs. (D) UMAP plots show cells from the first replicate of wild-type scRNA-seq data of Legoux et al. (a mixture of male and female MAITs), which are colored by signature scores defined by our cell cluster of MAITs (M1 ~ M8), signature gene sets (MAIT0, MAIT1, MAIT17b) of Legoux et al (MAIT0, MAIT1 and MAIT17b), and new cell clusters ('Cluster'). Low-quality cells with greater than 4% of UMIs assigned to mitochondrial genes were removed. HVGs were identified using the decomposeVar function of the scran package with  $FDR \leq 0.05$  and biological variability  $> 0.05$ . Clusters were found using the FindClusters function of the Seurat package on the first 50 PCs of HVGs with resolution = 2.0.

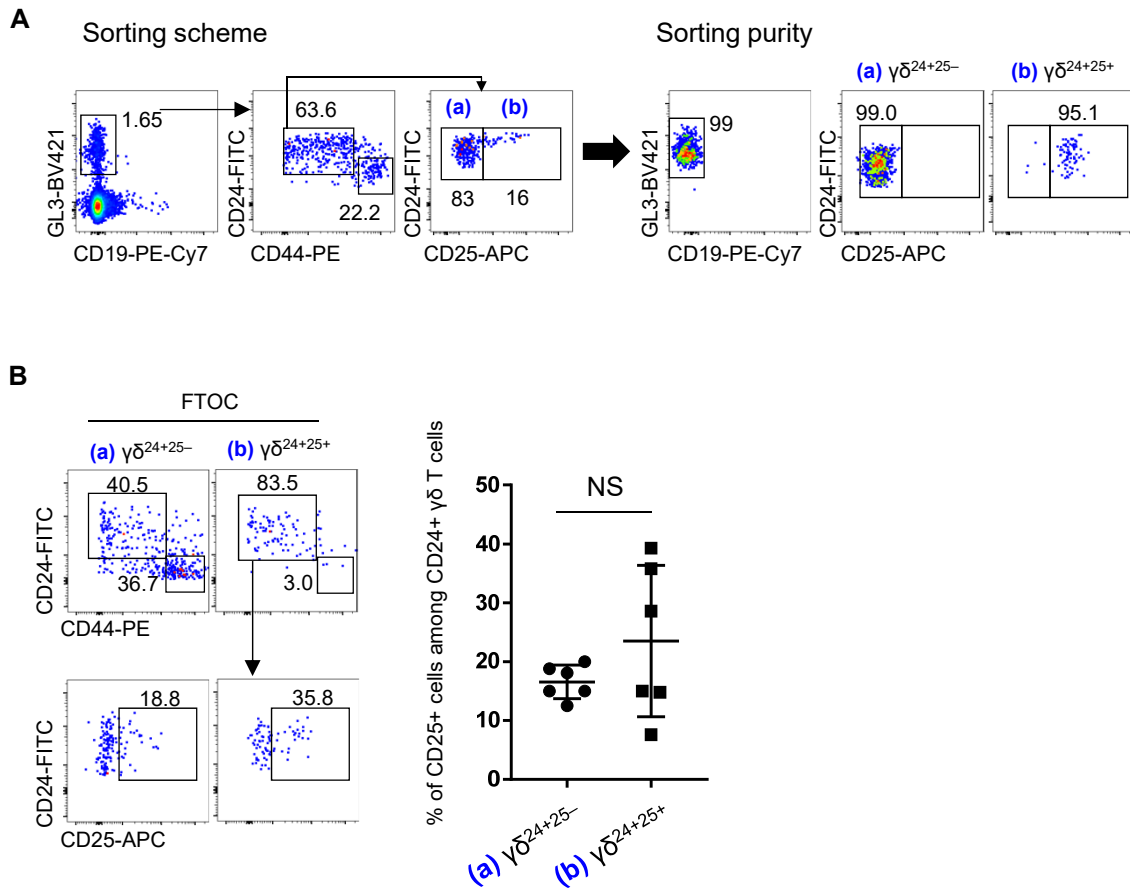


**Supplementary Figure 12. Validation of inferred differentiation trajectories of MAIT and  $\gamma\delta$  T cells.** UMAP plots showing differentiation trajectories of  $\gamma\delta$  T (A) and MAIT cells (B) by Monocle3. Cells were colored by clusters.



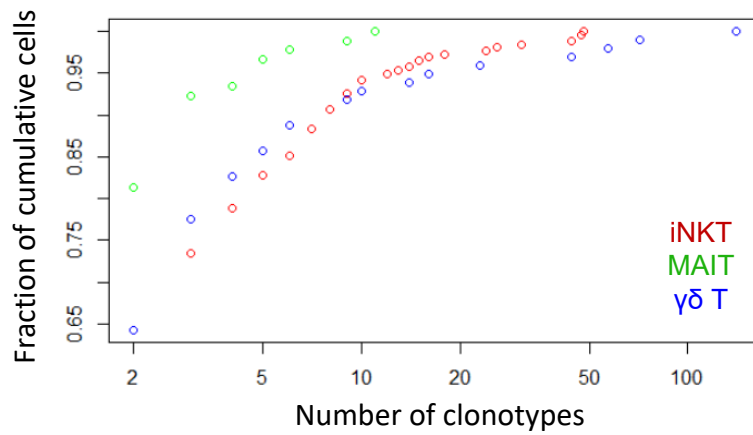
**Supplementary Figure 13. Correlation between NKT and MAIT subsets.** Graphs show signature scores of each NKT cluster in each MAIT cluster.





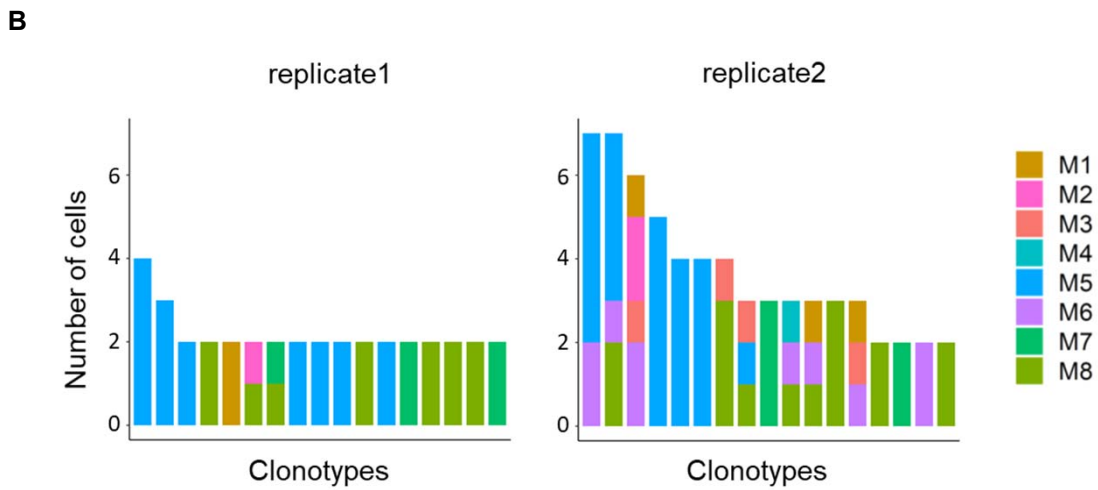
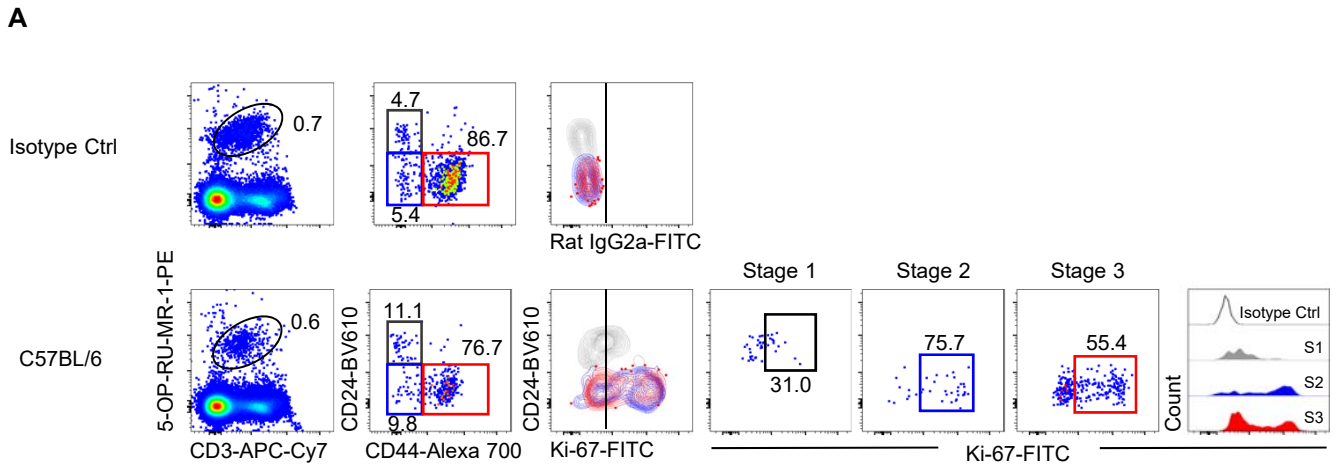
**Supplementary Figure 14.  $\gamma\delta^{24+25-}$  cells give rise to  $\gamma\delta^{24+25+}$  cells in FTOC experiment.**  $\gamma\delta^{24+25-}$  and  $\gamma\delta^{24+25+}$  cells were sorted from neonatal thymi of B6 mice and cultured in FTOC for 5 days. (A) Dot plots show sorting scheme and representative sorting purities. (B) Dot plots show the frequency of CD24<sup>+</sup>CD25<sup>+</sup> cells among CD24<sup>+</sup>  $\gamma\delta$  T cells after FTOC experiments in each group (left). Graph shows the frequencies of CD24<sup>+</sup>CD25<sup>+</sup> cells generated from  $\gamma\delta^{24+25-}$  (a, n=6) and  $\gamma\delta^{24+25+}$  (b, n=6). Results were pooled from four independent experiments. Numbers indicate frequencies of cells in adjacent gates. Data are presented as mean values  $\pm$  SD. Unpaired two-tailed *t*-tests were used for data analysis. \**P*<0.05. NS, not significant. Source data are provided as a Source Data file.

### Cumulative Distribution Function (clonotype > 1)

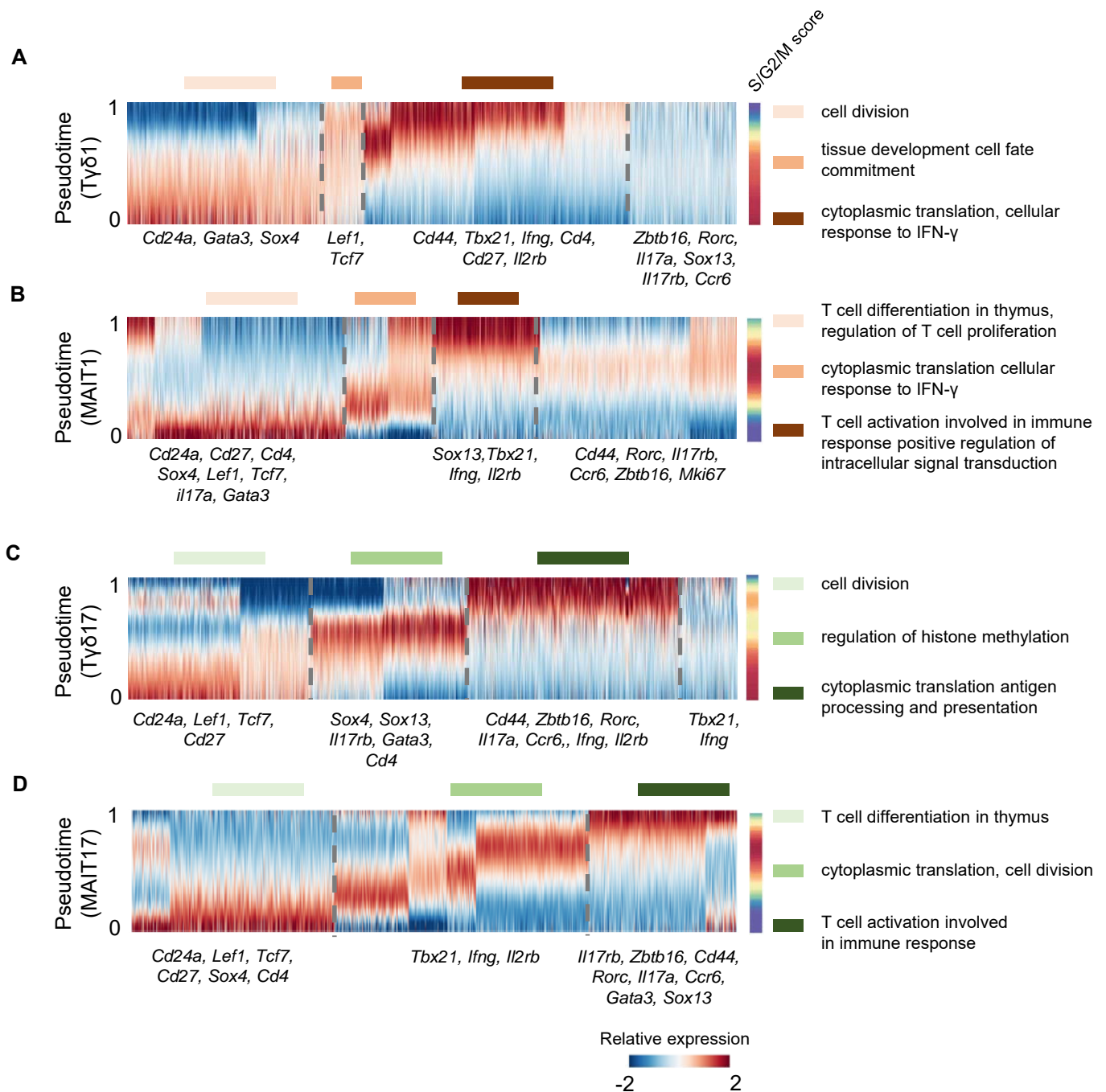


KS test	NKT-γδ T	γδ T-MAIT	NKT-MAIT
P value (Bonferroni)	1.000	0.388	0.001

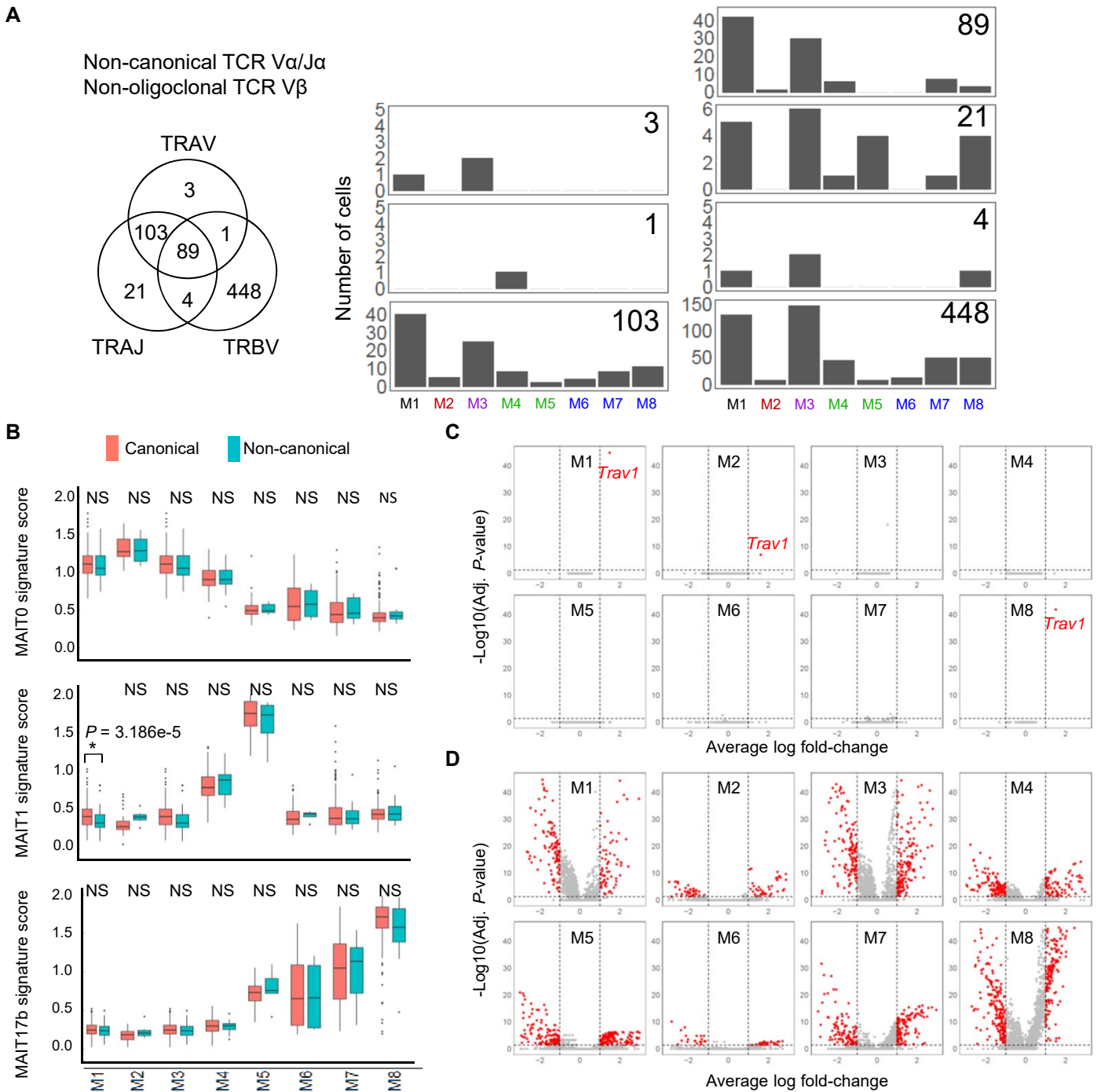
**Supplementary Figure 15. MAIT cells are more oligoclonal than iNKT or γδ T cells.** Graph shows fraction of cumulative cells repeated more than once from Figure 4C. Table shows statistical analysis (two-sided Kolmogorov-Smirnov tests).



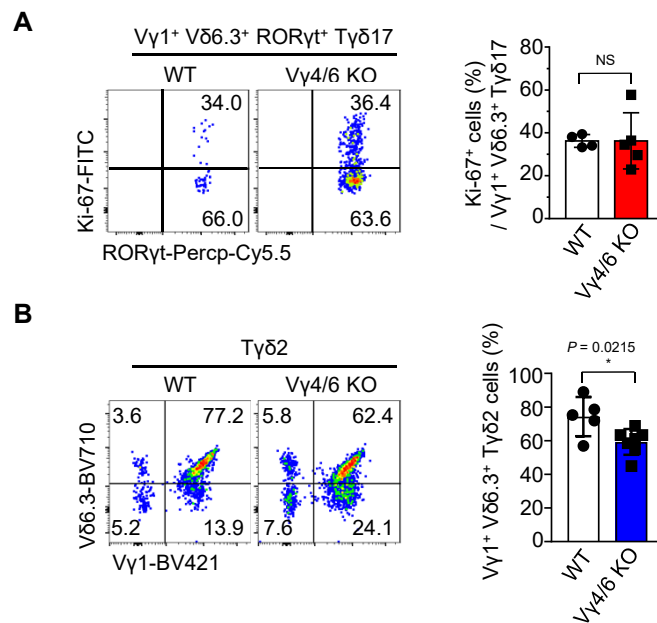
**Supplementary Figure 16. Ki-67 expression and clonal repeat of MAIT cells.** (A) Total thymocytes were enriched with MAITs and dot plots and histogram shows for their expression of Ki-67 in each stage. Representative results are from four independent experiments. (B) Bar plots show the ordered number of cells for each clonotype repeated 2 or more in each replicate of MAIT cells colored by UMAP regions. Each bar represents an individual clonotype.



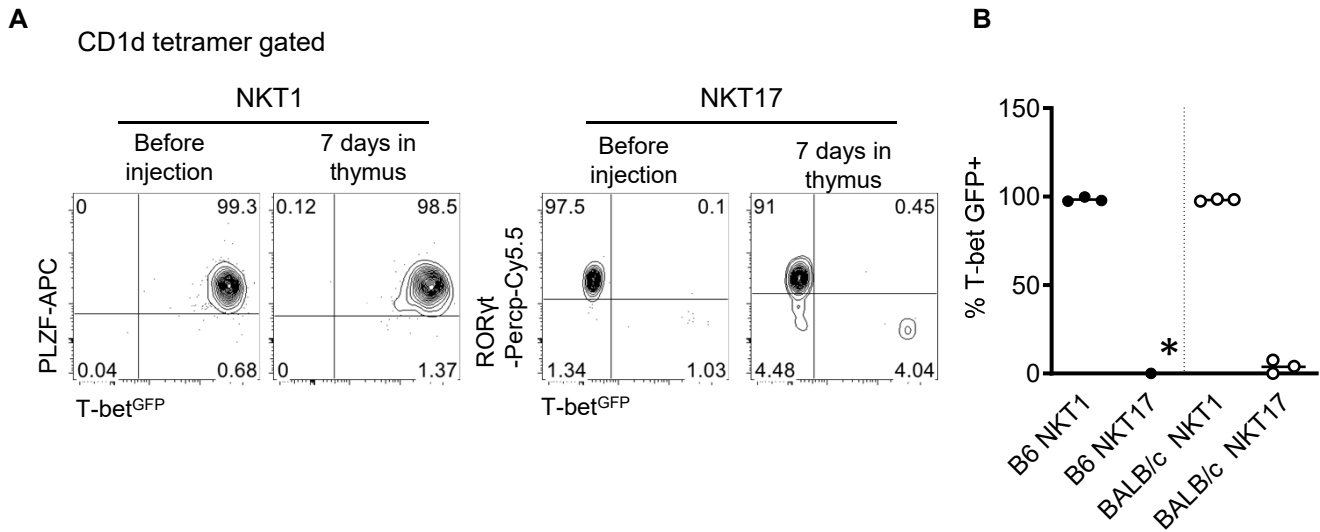
**Supplementary Figure 17. Single-cell trajectory analysis of MAIT and  $\gamma\delta$  T cells.** (A-D) Heat map illustrates gene expression trends of a union of marker genes of each cluster and subtype along differentiation trajectory towards T $\gamma\delta$ 1 (A), MAIT1 (B), T $\gamma\delta$ 17 (C) and MAIT17 (D). The enriched GO terms for each gene cluster separated by dashed gray lines are listed in the right panel. The S/G2/M cell cycle scores along the pseudotime trajectory, defined by the Z-score of the mean expression level of S/G2/M cell cycle related genes (Supplementary table 2), are shown in the graph.



**Supplementary Figure 18. Comparison between canonical and non-canonical MAIT cells.** (A) Total 669 non-canonical and/or non-oligoclonal MAIT TCRs were analyzed and Venn-diagram shows numbers of cells with indicated TCRs. Graphs show the distribution of non-canonical and/or non-oligoclonal cells in each cluster, and each region of Venn-diagram can be matched with same cell numbers in the graphs. (B) Box plots show expression of MAIT0, MAIT1 and MAIT17b signature genes obtained from Legoux et. al. (Ref #13) in 1892 MAIT cells examined over 2 replicates with canonical and non-canonical TCRs in each cluster. \* $P < 0.01$ ; NS, non-significant ( $P > 0.01$ , two-sided Wilcoxon rank sum test). Inside the boxplot, the black line represents the median value and the size of the box is determined by the 25th and 75th percentiles of the data. The length of the whiskers is 1.5 times of IQR(Interquartile range). (C) Volcano plots showing differential gene expression profile between MAITs with canonical and non-canonical TCRs for each cell cluster of MAITs. (D) Volcano plots show differential gene expression profiles between MAITs with canonical TCRs and randomly selected CD4<sup>+</sup>/CD8<sup>+</sup> DP cells (as a potential source of contamination of cells) in each cell cluster of MAITs. Differentially expressed genes (adjusted P-value  $< 0.05$ , log fold-change  $> 1$ , two-sided Wilcoxon rank sum test) are highlighted in red (C-D).



**Supplementary Figure 19. Tγδ17 cells in WT and Vγ4/6 deficient mice.** (A) Representative dot plots show Ki-67 expressions on CD24<sup>low</sup> Vγ1<sup>+</sup> Vδ6.3<sup>+</sup> RORγt<sup>+</sup> Tγδ17 cells from WT (left, n=4) or Vγ4/6 KO (right, n=5) mice and graph shows statistical analysis. Results are pooled from four independent experiments. (B) Representative dot plots show frequencies of Vγ1<sup>+</sup> Vδ6.3<sup>+</sup> cells among CD24<sup>low</sup> PLZF<sup>high</sup> Tγδ2 cells from WT (left, n=5) or Vγ4/6 KO (right, n=7) and graph shows statistical analysis. Representative results pooled from four independents. Numbers indicate frequencies of cells in adjacent gates. Data are presented as mean values ± SD. Unpaired two-tailed *t*-tests were used for data analysis. \**P*<0.05. NS, not significant. Source data are provided as a Source Data file.



**Supplementary Figure 20. NKT1 and NKT17 cells are terminally differentiated population.** (A) Total thymocytes from either from B6 or BALB/c mice were enriched with CD1d tetramer and sorted as NKT1 (Tbx21<sup>gfp+</sup>) and NKT17 (Tbx21<sup>gfp-</sup> CD4<sup>-</sup>) cells and stained with transcription factors before intrathymic injections. Sorted live cells were injected into congenic host and analyzed after 7 days. Representative plots show the phenotype of cells before and after injection of each population. Representative data of 3 independent experiments are shown. (B) Graph shows statistical analysis of GFP+ cells in donor population (N=3). \*, two mice did not contain donor NKT cells. Source data are provided as a Source Data file.

		Total cells	TCR analysis
NKT	N1	225	202
	N2	210	188
	N3	843	769
	N4	785	657
	N5	871	690
	N6	68	22
	N7	283	247
	Total	3285	2775
MAIT	M1	532	440
	M2	83	48
	M3	562	494
	M4	154	134
	M5	148	137
	M6	113	106
	M7	231	209
	Total	2287	1892
γδ T	G1	308	201
	G2	334	218
	G3	295	184
	G4	741	461
	G5	267	143
	G6-1	155	101
	G6-2	74	68
	G7-1	417	232
	G7-2	76	57
Total	2667	1665	
Total		8239	6332

Supplementary Table 1. Number of cells analyzed.



S phase genes	G2/M phase genes
<i>Dnajc2</i>	<i>Dnajc2</i>
<i>Mcm2</i>	<i>Chek1</i>
<i>Mcm3</i>	<i>Ppm1d</i>
<i>Mcm4</i>	<i>Brca2</i>
<i>Mki67</i>	<i>Ccna1</i>
<i>Mre11a</i>	<i>Ccnb1</i>
<i>Msh2</i>	<i>Cdc25a</i>
<i>Pcna</i>	<i>Cdc25b</i>
<i>Rad17</i>	<i>Cdk2</i>
<i>Rad51</i>	<i>Nek2</i>
<i>Sumo1</i>	<i>Npm2</i>
	<i>Pes1</i>
	<i>Prm1</i>
	<i>Rad21</i>
	<i>Ran</i>
	<i>Shc1</i>
	<i>Smc1a</i>
	<i>Stag1</i>
	<i>Terf1</i>
	<i>Psmg2</i>
	<i>Wee1</i>

**Supplementary Table 2. List of cell cycle related genes.**